Observed and Simulated Cirrus Cloud Properties at the SGP CART Site

A. D. Del Genio and A. B. Wolf
National Aeronautics and Space Administration
Goddard Institute for Space Studies
New York, New York

G. G. Mace
University of Utah
Salt Lake City, Utah

Introduction

Despite their potential importance in a long-term climate change, less is known about cirrus clouds than most other cloud types, for a variety of reasons (Del Genio 2001) including: (1) the difficulty of remotely sensing ice water content (IWC), (2) uncertainty in the identities of ice nuclei and the relative importance of different nucleation processes, (3) significant variations in depth and optical thickness caused by formation and sedimentation of large particles, and (4) our relatively poor documentation of the dynamics of the upper troposphere. Aircraft observations suggest that the sub-grid variability of cirrus microphysical properties might be modeled using an approach similar to that for marine stratus clouds (Smith and Del Genio 2001a). Those data represent a very limited sample, however, and leave open the question of how cirrus radiative properties might be predicted given knowledge of their microphysical characteristics.

Recently, though, the advent of the millimeter cloud radar (MMCR) has made it feasible to develop long-term surface-based climatologies of cirrus properties. Mace et al. (1998) have developed techniques for retrieving cirrus cloud boundaries, IWC, effective radius (r_e), and number concentration from MMCR reflectivities combined with atmospheric emitted radiance interferometer (AERI) downwelling radiances and have applied the algorithm to almost two years of MMCR data (11/96-5/98) at the Atmospheric Radiation Measurement (ARM) Program Southern Great Plains (SGP) Cloud and Radiation Testbed (CART) site. Three-minute mean retrievals are available at 8-minute intervals for isolated cirrus (i.e., no simultaneous low- or mid-level clouds) at temperatures < -20°C. In this paper we document some of the statistical properties of the observed cirrus and their sensitivity to environmental conditions and determine relationships between cirrus radiative and microphysical properties. We also compare the results for convectively generated summer cirrus to synoptically forced winter cirrus, and we test the ability of the Goddard Institute for Space Studies (GISS) stratiform cloud parameterization to reproduce some of the observed relationships by conducting single-column model (SCM) tests.

Considine et al. (1997) presented a simple conceptual model to predict the cloud cover and probability density function (PDF) of liquid water path (LWP) for marine stratus clouds. The model was based on an assumed Gaussian distribution of cloud depths controlled by turbulent vertical velocities and

associated fluctuations of temperature and humidity. Smith and Del Genio (2001a) showed that aircraft-observed mid-latitude cirrus clouds could be described in a similar way if ice sedimentation effects on cloud depth were taken into account. The 19 months of MMCR data permit a much more robust statistical sample. The disadvantage of the SGP retrievals is that AERI observes for only 3 of every 8 minutes, with the MMCR sampling every 30 seconds, so it is not possible to construct PDFs for individual cirrus. Instead, we aggregate the 3-minute mean retrievals into 2 subsets: An "overcast" population of all retrievals during times when isolated cirrus were observed for at least 1 hour (implying cloudiness over at least ~100 km for typical upper troposphere wind speeds) and a "not overcast" population of all other points. The 19-month aggregate ice water path (IWP) PDFs for the two subsets (not shown) exhibit behavior similar to that observed by Smith and Del Genio, with the mode value of IWP shifting away from the lowest IWP bin as conditions change from partly cloudy to overcast. This is consistent with the conceptual model described above.

Since general circulation models (GCMs) predict only gridbox mean IWC and cloud depth (D) and parameterize gridbox means of other quantities such as r_e, number concentration (N) and optical thickness (τ) as a function of predicted variables, sub-grid variability must be characterized in terms of the mean cloud properties or environmental conditions predicted by the GCM. For most cirrus properties, their standard deviation tends to be ~2/3-3/4 the mean value, especially for thinner cirrus cases, consistent with the results of Smith and Del Genio (2001b). For thicker cirrus, variability appears to level off and become independent of further increases in the mean. Whether this limitation is real or a consequence of decreasing sensitivity of the retrievals, as cirrus emittances approach 1 is not known. The worst case is for cloud depth, whose standard deviation shows only a weak relationship to its mean value. Furthermore, for cirrus, where sedimentation extends cloud base downward from the original altitude where saturated lifting began, cloud depth is not controlled strictly by the dynamics.

Figure 1 compares radar retrievals of actual cloud depth D to radiosonde estimates of the "generating layer depth" D_G, defined as the continuous distance from the first point above cloud base at which a nearly coincident sounding indicates ice saturation up to the point at which the relative humidity drops below ice saturation. This is assumed to represent the original lifted layer in which the cirrus formed. Despite the inadequacies of sonde humidity measurements in the upper troposphere, the soundings are well fit by a relationship of the form $D = D_G + 500$ m. This suggests at the least that GCM parameterizations of cirrus fallspeed and sublimation require no more complexity than that required to ensure that all ice removed from cirrus cloud base sublimes completely within 1 to 2 layers below cloud base (given that even the highest resolution GCMs only have a resolution of ~500 m in the upper troposphere). Cloud depth variability is more difficult to characterize. In principle, we might expect less stable environments to allow lifting over greater depths and more vigorous turbulence, resulting in thicker clouds with greater cloud depth variability. However, standard deviations of D show only a weak decrease with increasing Richardson number (not shown).

Given a GCM prediction of IWC and D, radiative properties such as τ can only be parameterized if a relationship for r_e in terms of other cloud or environmental properties exists. Figure 2 shows mean r_e as functions of temperature (T) and each of three other cloud parameters (N, D, IWC). N decreases with T; r_e is a strong function of N, but not solely, because IWC increases with mean cloud T. D also increases with mean cloud T, indicating that there is more variability in cirrus cloud base height than top height. While r_e increases with T for a given D, it also increases with D for a given T. This is consistent with

the simple model picture of cirrus generation by adiabatic lifting—the greater the D_G, the more ice is formed and the larger r_e is for a given N. IWC increases with T, but with much scatter. The upper boundary of the main cloud of points is fit approximately by a function $f = (IWC)^{-1}d(IWC)/dT \approx .07\text{-}.09$ K^{-1}, close to the adiabatic value. Most points fall beneath this curve, an expected result given the important ice sink due to sedimentation. For a given T, r_e increases with IWC, as explained above, but for a given IWC r_e also increases with T despite the fact that D must decrease with increasing T at fixed IWC. This indicates that the decrease of N with increasing T is most responsible for the large particle sizes at warm temperatures.

Early cloud models used a temperature-dependent parameterization of N by Fletcher (1962), but recent evidence suggests that this formula greatly underpredicts ice concentrations at warm temperatures. More recently, Meyers et al. (1992) argued from cloud chamber experiments that ice deposition and freezing nucleation could be represented instead as an increasing function of ice supersaturation. This parameterization is now commonly used to predict cirrus particle sizes in cloud models and in at least one GCM (Rotstayn et al. 2000), despite the fact that it strictly applies only on small scales. We collected all retrievals of N that occurred within 2 minutes of the time a sounding passed through the indicated cloud altitude. Figure 3 shows that cloud layer mean N does not increase with cloud mean relative humidity. The situation does not change if we restrict the comparison to the mean humidity over the generating layer (which contains only points supersaturated with respect to ice) or if we use the maximum relative humidity instead. Figure 4 compares the MMCR/AERI retrievals to the Fletcher formula, the Meyers et al. scheme using observed relative humidities (calculating N at each height and then averaging N over cloud depth), and the Meyers et al. formula assuming water saturation (as implemented by Rotstayn et al. in their GCM), and ice saturation. If the retrievals of N are accurate to within 1-2 orders of magnitude, then none of these parameterizations comes close to capturing either the mean N or its T dependence. Of course, the cold temperature bias and finite response time of the sonde humidity sensors (Miloshevich et al. 2001) introduces errors that might explain the disagreement between the retrieved N and that predicted by Meyers et al.; this highlights the need for improved upper troposphere humidity measurements. Taken at face value, the errors in parameterized N imply a particle size (and thus optical thickness) error of a factor of 2 or more for a model that correctly predicts IWC and D. Currently, the GISS GCM assumes a constant value of $N = 6 \times 10^4$ m^{-3}, which does a reasonable job at warm temperatures but does not capture the increase of N at cold temperatures. Given the accuracy of available humidity data, there is really no way to properly test the relationship of the Meyers et al. parameterization to large-scale cirrus behavior, and perhaps the best short-term strategy for GCM parameterization would be an empirical fit to the temperature dependence of N in Figure 4 if similar behavior can be observed in other climate regimes.

Given a PDF of IWC, the radiative impact of cirrus cannot be calculated unless an equivalent pdf of radiative properties can be estimated. One approach might be to construct joint distributions of IWC and either r_e or N. Heymsfield and McFarquhar (1996) take a simpler approach, showing that for tropical cirrus, cloud extinction (β) closely follows the relationship $\beta = C(IWC)^n$, with $n \sim 0.8\text{-}0.9$. Figure 5 shows that τ follows a power-law increase with IWC with a slope near or slightly > 1 at the SGP in both summer and winter. Thus, the seasonal difference in the dynamical source of cirrus seems to have little effect on this aspect of cloud properties at the SGP. On the other hand, Mace et al. (2001) notice systematic differences between TWP and SGP cirrus properties, the source of which has not yet been isolated. Figures 6 and 7 show that the nearly linear dependence of τ on IWC arises because both

D and r_e vary with IWC at similar rates. The r_e-IWC regressions have somewhat different slopes in summer and winter because of the presence of a second population of points, mostly in summer, for which r_e decreases with IWC and N (not shown) increases strongly with IWC. A few of these points are at cloud edges and may be partly cloud-filled. All clouds that have cloud base T < -40°C fall along this anomalous curve, but not all the points that fall along this curve extend up to the -40°C level. Whatever their explanation, when these points are removed, the r_e-IWC regression for the remaining points is similar to that for the winter case.

Analogous results for a simulation of the Summer 1997 IOP with the GISS SCM are also shown in Figures 5-7. The SCM has a main population of points that falls along a line for which n = 2/3, consistent with the SCM's assumption of constant N and $r_e \propto (\mathrm{IWC})^{1/3}$. However, a scattering of other points with much higher and lower τ values exists. The lower panel of Figure 7 shows that this occurs because the 19-layer SCM's coarse vertical resolution in the upper troposphere (> 1 km) results in a sub-population of single-layer cirrus whose depths are necessarily independent of IWC. Thus, D (and τ) variations with IWC in the SCM are muted relative to what is observed. This argues that climate models need to accommodate at least 30 layers in the troposphere to have a reasonable chance of simulating variability in cirrus radiative properties.

Corresponding Author

Anthony D. Del Genio, adelgenio@giss.nasa.gov, (212) 678-5588

References

Considine, G., J. A. Curry, and B. Wielicki, 1997: Modeling cloud fraction and horizontal variability in marine boundary layer clouds. *J. Geophys. Res.*, **102**, 13,517-13,525.

Del Genio, A. D., 2001: GCM simulations of cirrus for climate studies. In *Cirrus,* D. K. Lynch, ed., Oxford University Press, 310-326.

Fletcher, N. H., 1962: *Physics of Rain Clouds*. Cambridge University Press, 386 pp.

Heymsfield, A. J., and G. M. McFarquhar, 1996: High albedos of cirrus in the tropical Pacific warm pool: Microphysical interpretations from CEPEX and from Kwajalein, Marshall Islands. *J. Atmos. Sci.*, **53**, 2424-2451.

Mace, G. G., T. P. Ackerman, P. Minnis, and D. F. Young, 1998: Cirrus layer microphysical properties derived from surface-based millimeter radar and infrared radiometer data. *J. Geophys. Res.*, **103**, 23,207-23,216.

Mace, G. G., E. N. Vernon, Y. Zhang, J. M. Comstock, and T. P. Ackerman, 2001: A comparison of tropical and mid-latitude cirrus microphysical properties using ARM data. This proceedings.

Meyers, M. P., P. J. DeMott, and W.R. Cotton, 1992: New primary ice-nucleation parameterizations in an explicit cloud model. *J. Appl. Meteor.*, **31**, 708-721.

Miloshevich, L. M., A. J. Heymsfield, and A. Paukkunen, 2001: Preliminary correction of Vaisala radiosonde humidity measurements for slow sensor time-response at cold temperatures. This proceedings.

Rotstayn, L. D., B. F. Ryan, and J. J. Katzfey, 2000: A scheme for calculation of the liquid fraction in mixed-phase stratiform clouds in large-scale models. *Mon. Wea. Rev.*, **28**, 10,070-1088.

Smith, S. A., and A. D. Del Genio, 2001a: A simple conceptual model of cirrus horizontal inhomogeneity and cloud fraction. *Quart. J. Roy. Meteor. Soc.* Submitted.

Smith, S. A., and A. D. Del Genio, 2001b: Analysis of aircraft, radiosonde, and radar observations in cirrus clouds observed during FIRE II: The interactions between environmental structure, turbulence, and cloud microphysical properties. *J. Atmos. Sci*, **58**, 451-461.

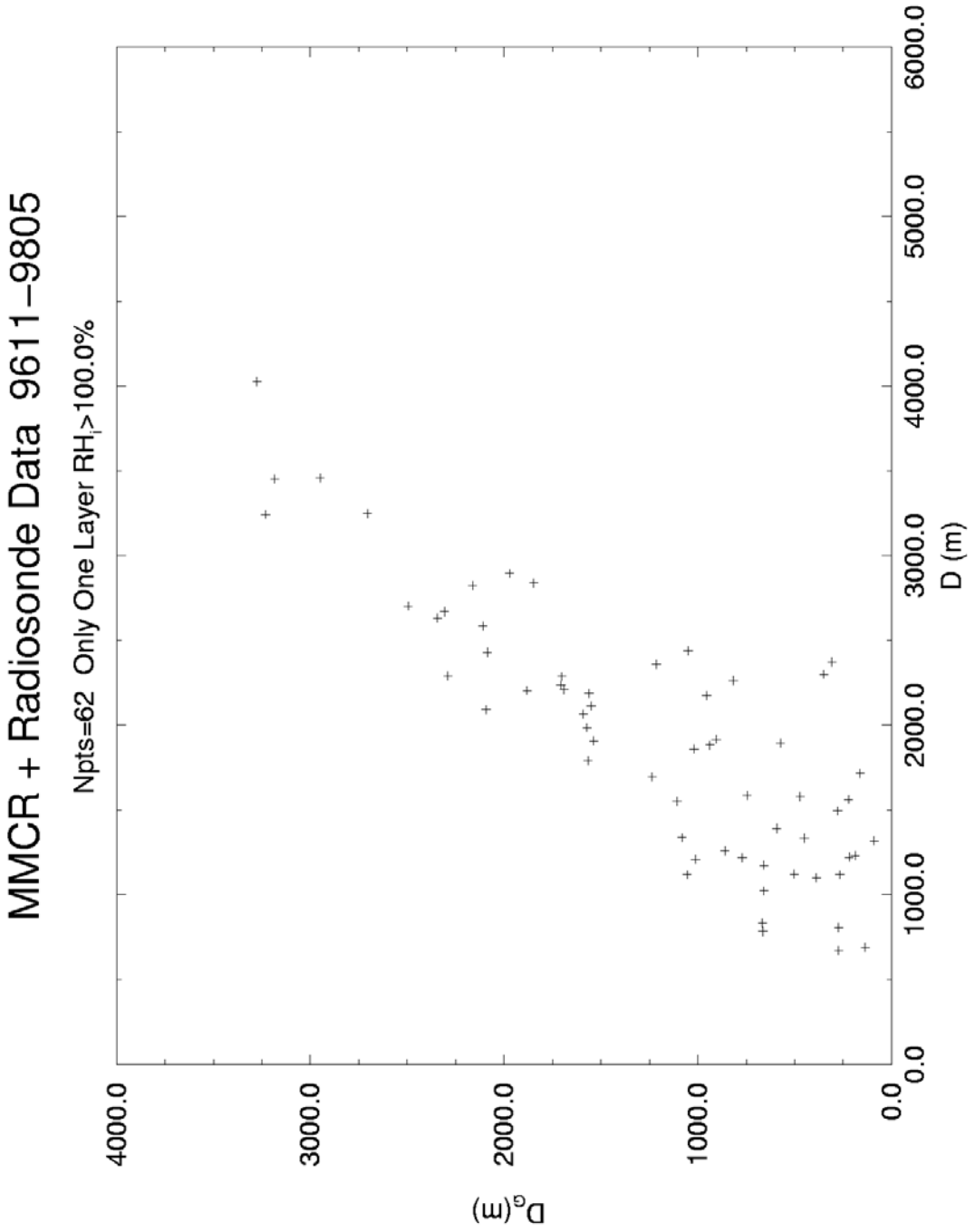

Figure 1. Cirrus layer generating depth (depth of the ice-supersaturated region in soundings) versus actual mean cirrus cloud depth (derived from millimeter radar retrievals) for all cases with single generating layers and at least 10 radar retrievals within 90 minutes of a sounding.

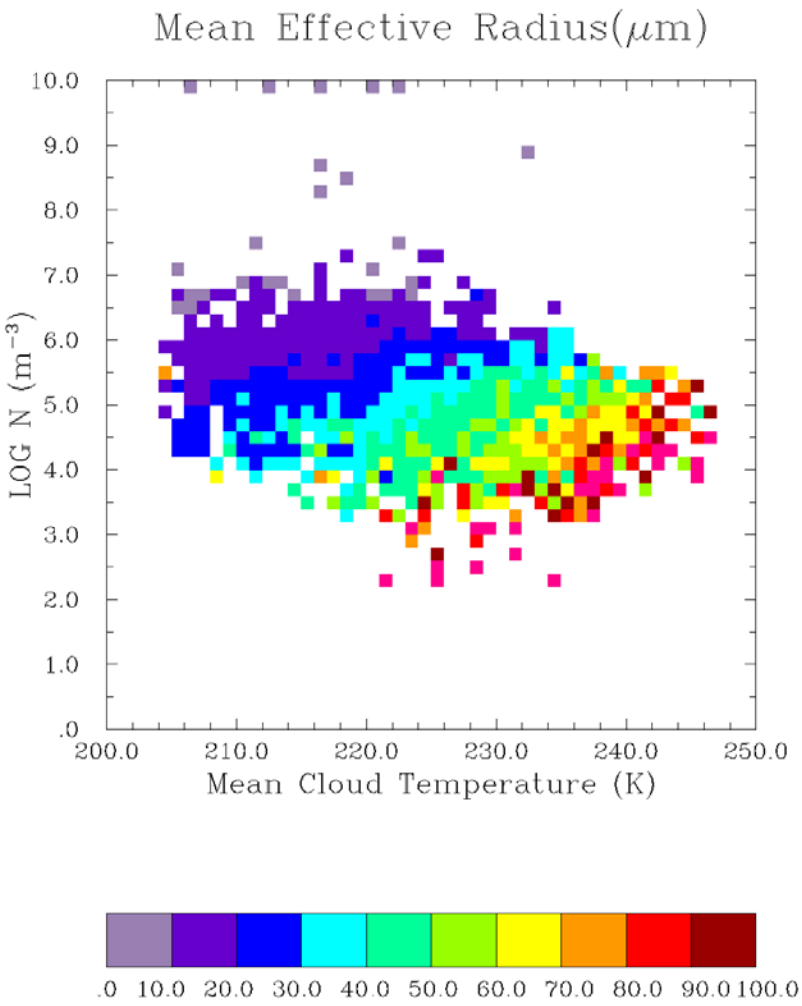

(a)

Figure 2. Two-dimensional distributions of cirrus crystal effective radius as functions of **(a) number concentration and temperature**, (b) cloud physical thickness and temperature, and (c) IWC and temperature.

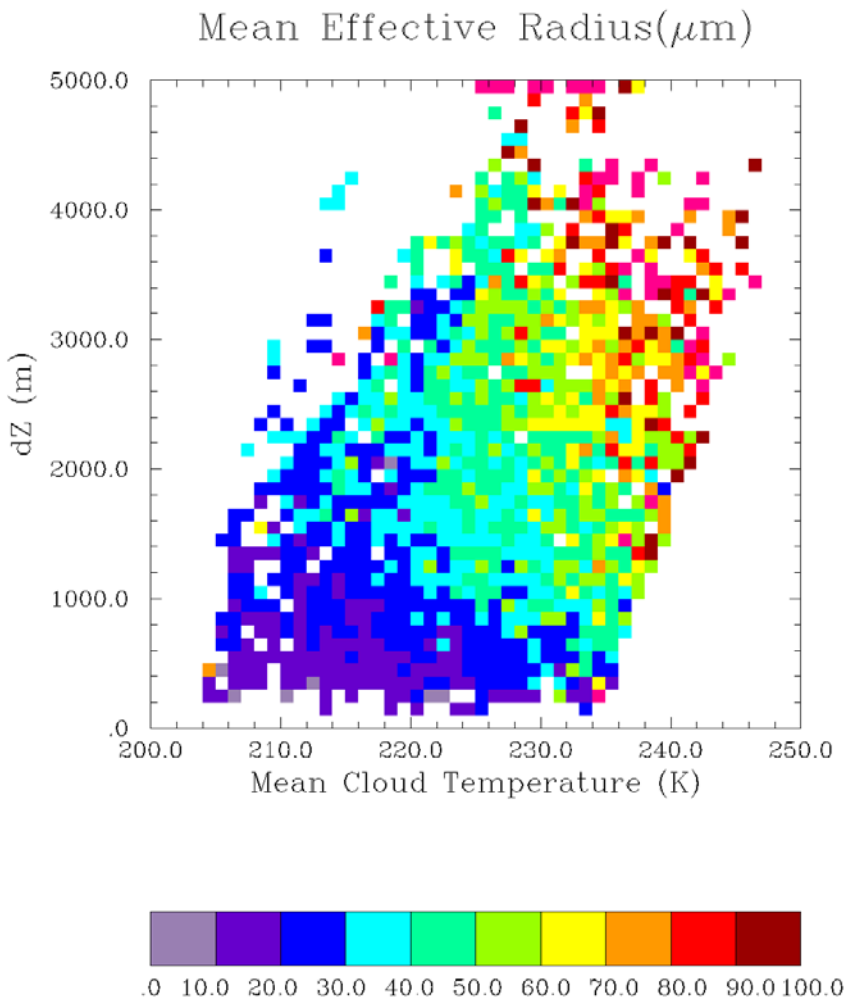

(b)

Figure 2 (contd). Two-dimensional distributions of cirrus crystal effective radius as functions of (a) number concentration and temperature, **(b) cloud physical thickness and temperature**, and (c) IWC and temperature.

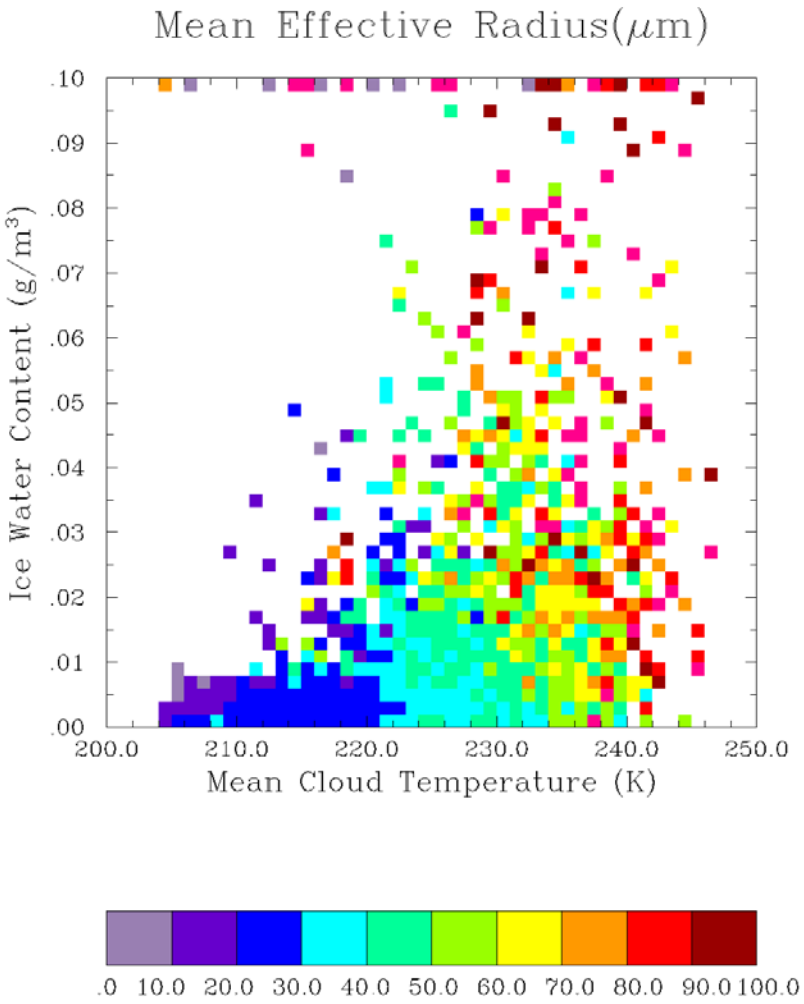

(c)

Figure 2 (contd). Two-dimensional distributions of cirrus crystal effective radius as functions of (a) number concentration and temperature, (b) cloud physical thickness and temperature, and **(c) IWC and temperature**.

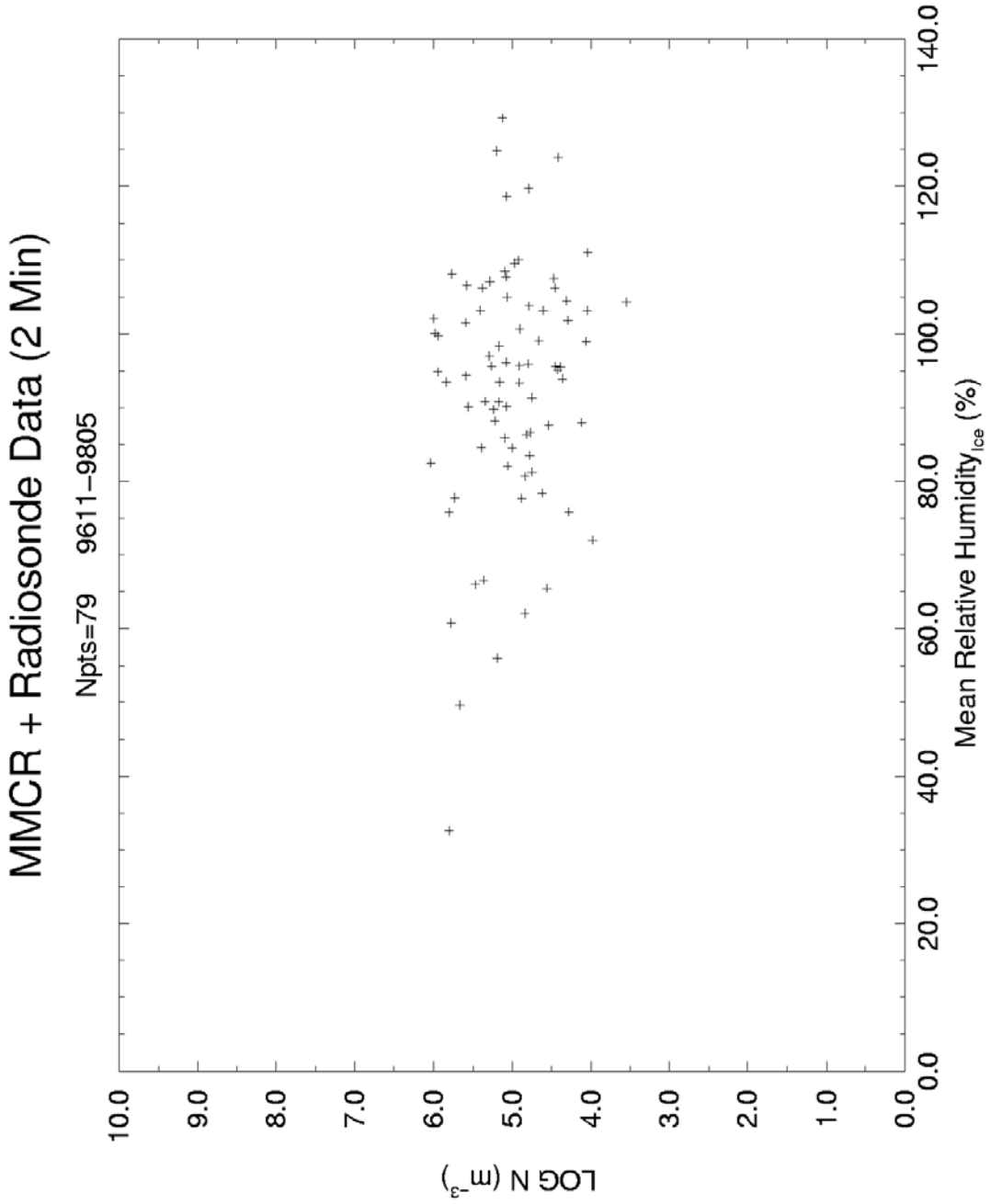

Figure 3. Cirrus crystal number concentration versus mean cloud layer relative humidity with respect to ice for all radar retrievals within 2 minutes of a sounding.

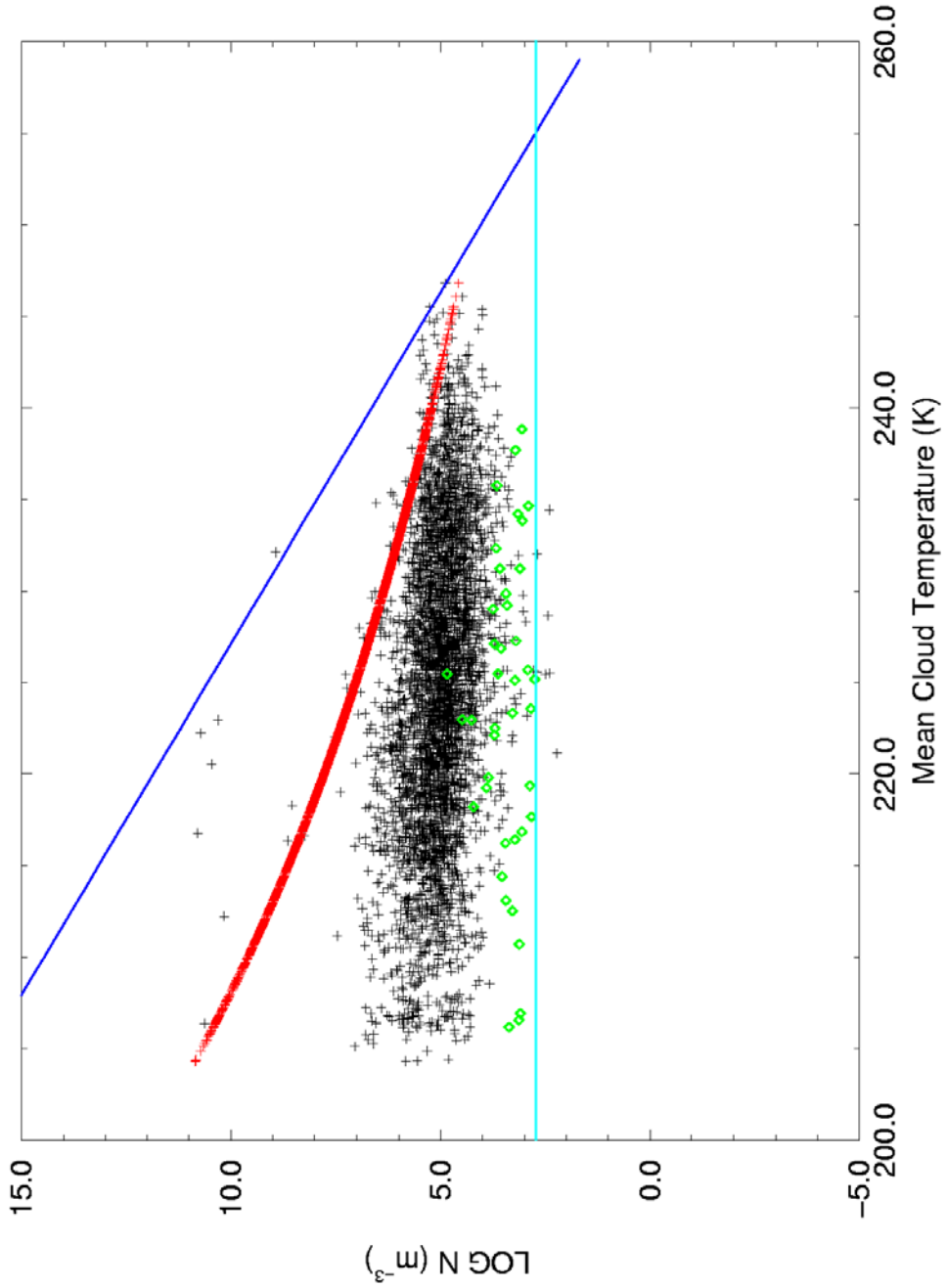

Figure 4. Comparisons of observed and theoretically predicted cirrus crystal number concentration as a function of cloud layer mean temperature. Black "+" signs: MMCR/AERI retrievals. Violet curve: Fletcher (1962) parameterization. Green diamonds: Meyers et al. (1992) parameterization. Red curve: Meyers et al. parameterization assuming water saturation. Light blue curve: Meyers et al. parameterization assuming ice saturation.

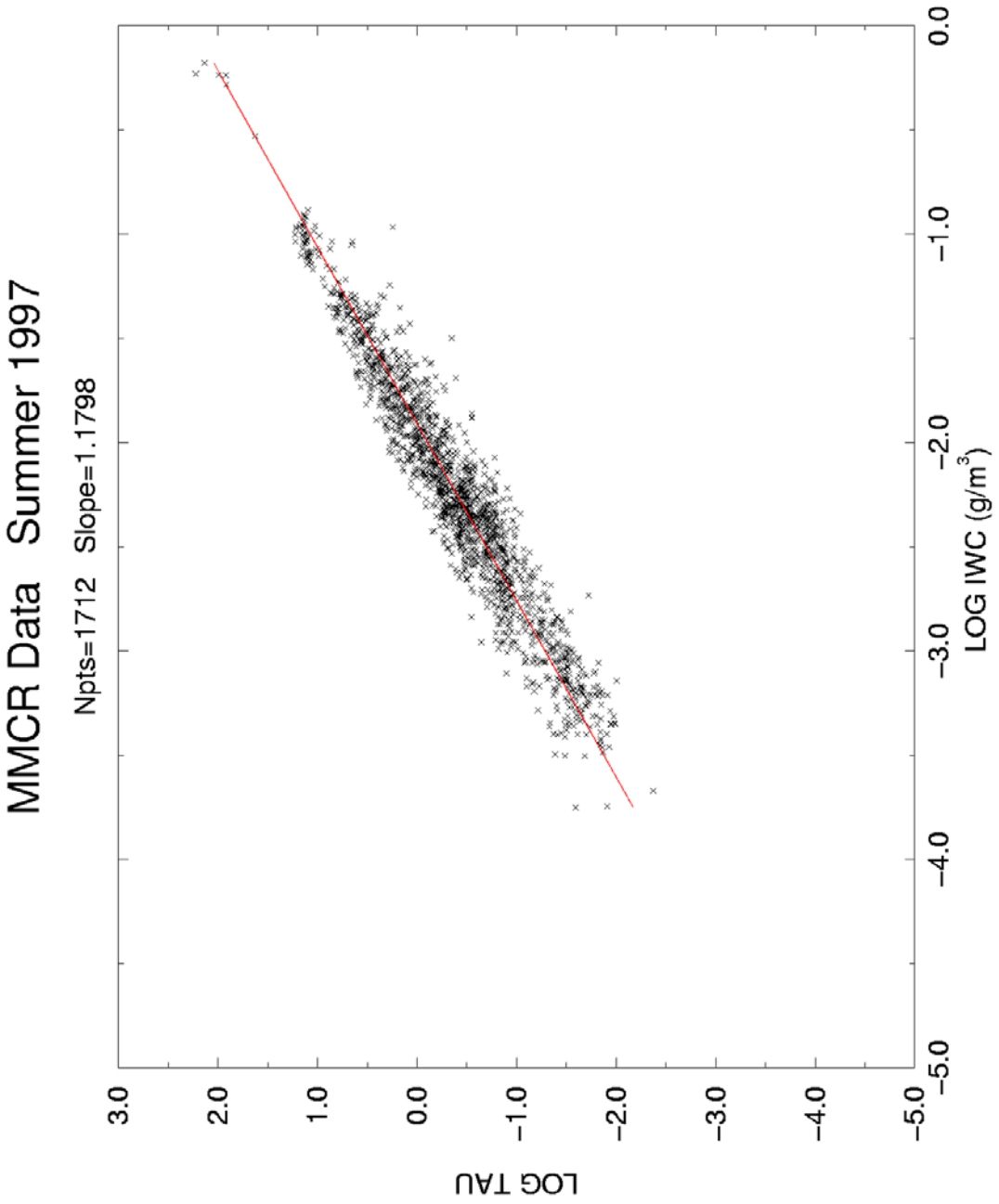

(a)

Figure 5. Cirrus visible optical thickness versus IWC for **(a) Summer 1997 SGP MMCR/AERI retrievals,** (b) Winter 1997-1998 SGP MMCR/AERI retrievals, and (c) Summer 1997 SGP simulation with the GISS SCM.

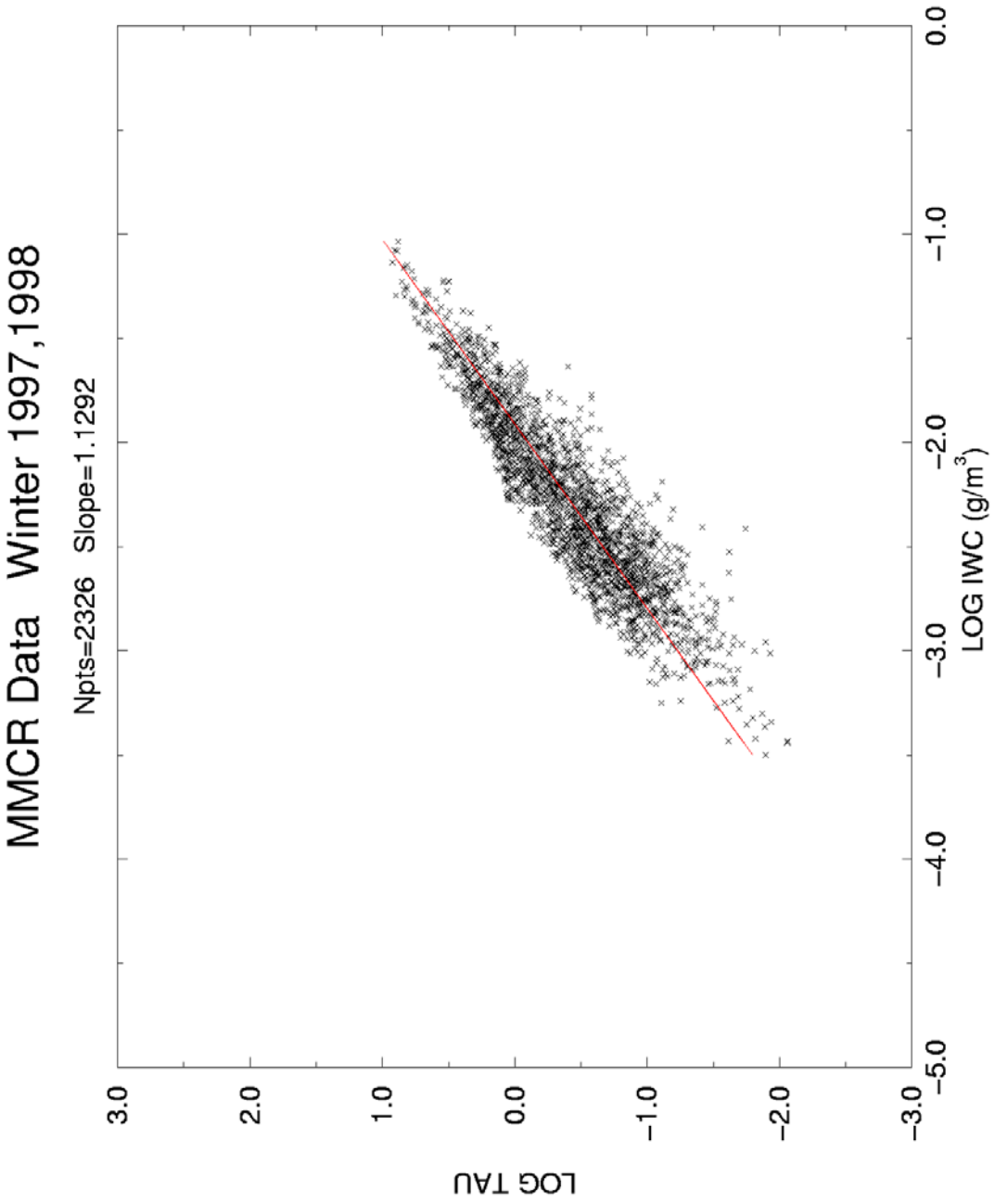

(b)

Figure 5 (contd). Cirrus visible optical thickness versus IWC for (a) Summer 1997 SGP MMCR/AERI retrievals, **(b) Winter 1997-1998 SGP MMCR/AERI retrievals,** and (c) Summer 1997 SGP simulation with the GISS SCM.

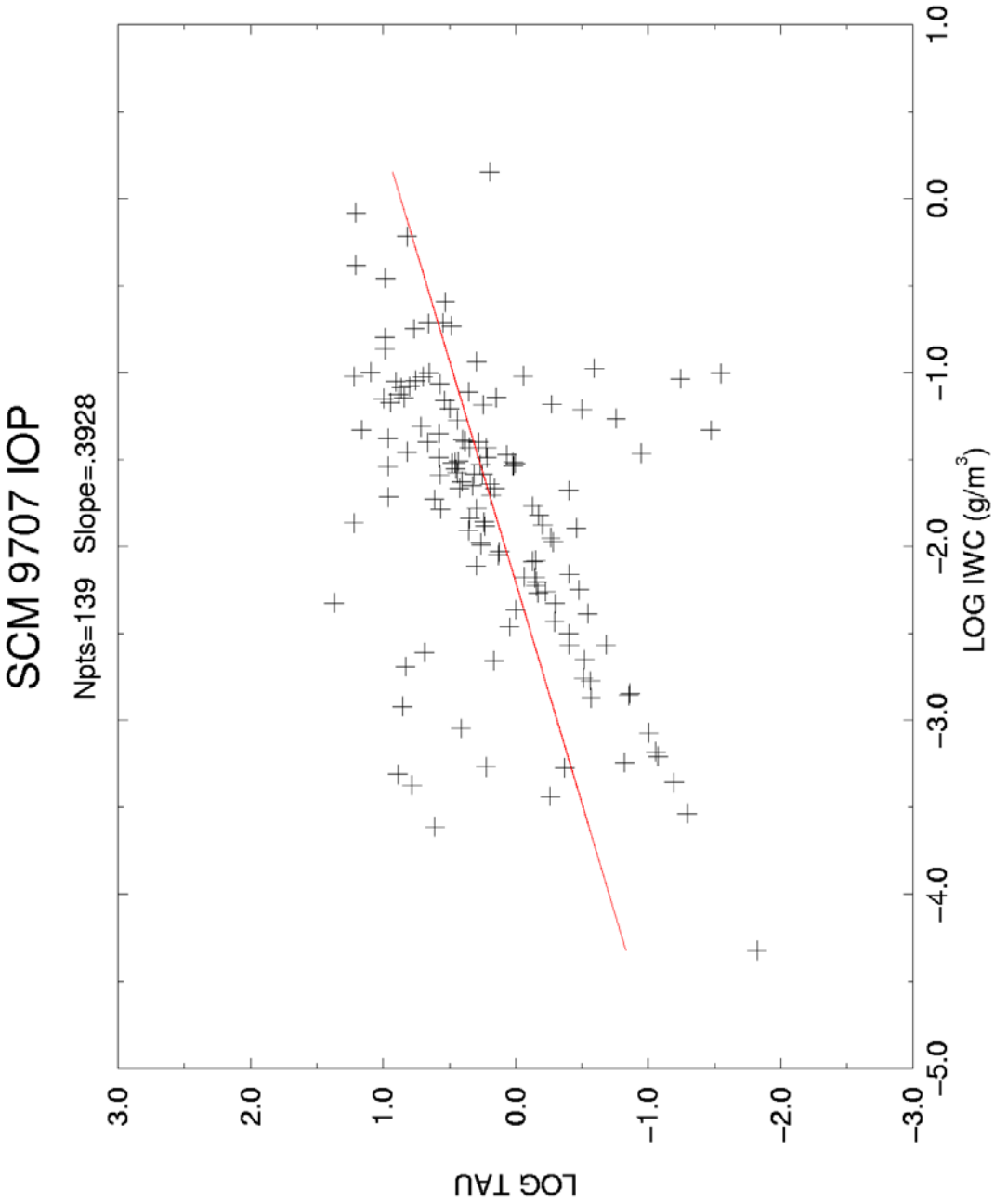

(c)

Figure 5 (contd). Cirrus visible optical thickness versus IWC for (a) Summer 1997 SGP MMCR/AERI retrievals, (b) Winter 1997-1998 SGP MMCR/AERI retrievals, and **(c) Summer 1997 SGP simulation with the GISS SCM**.

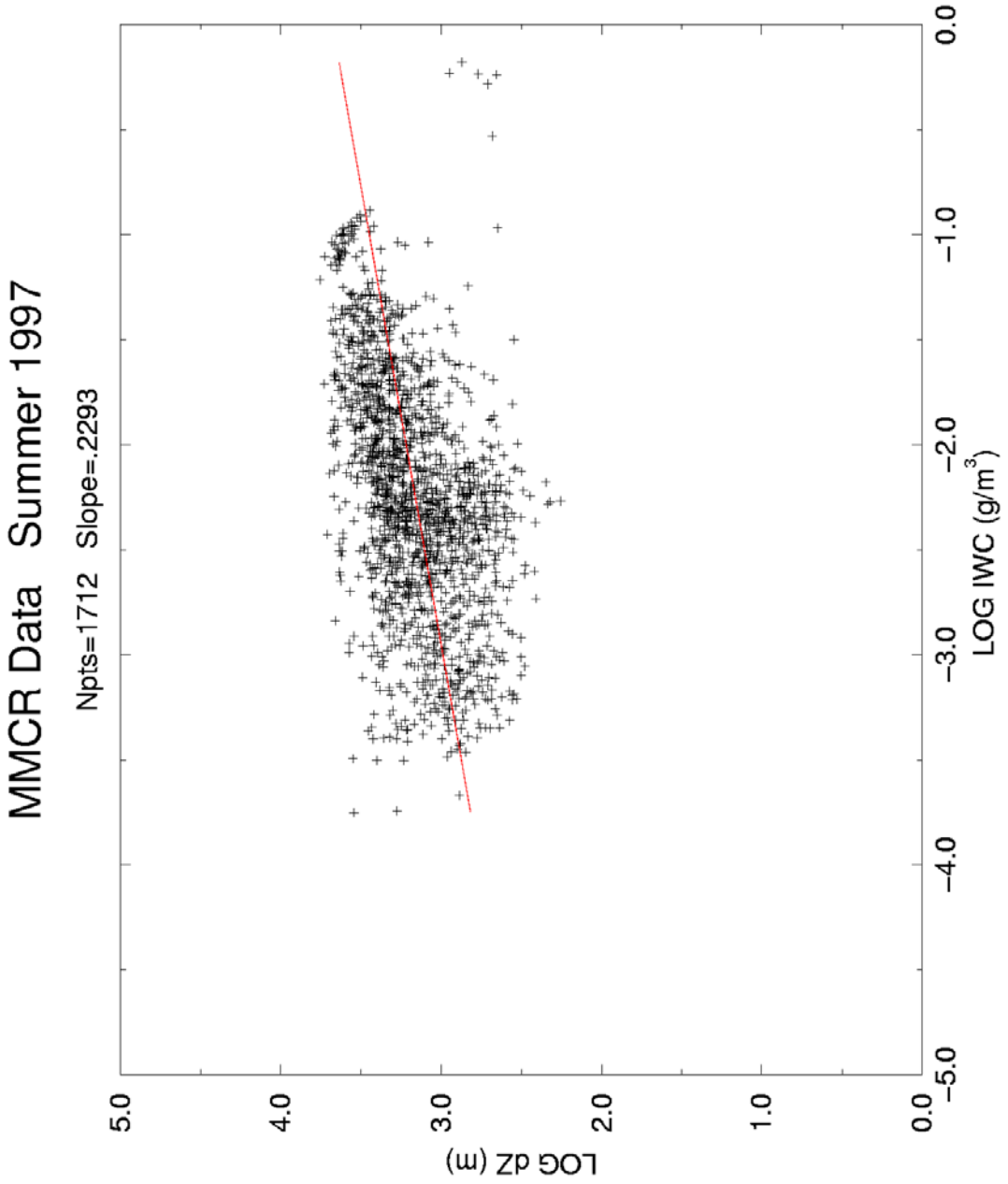

Figure 6(a). As in Figure 5a but for cirrus cloud physical thickness versus IWC.

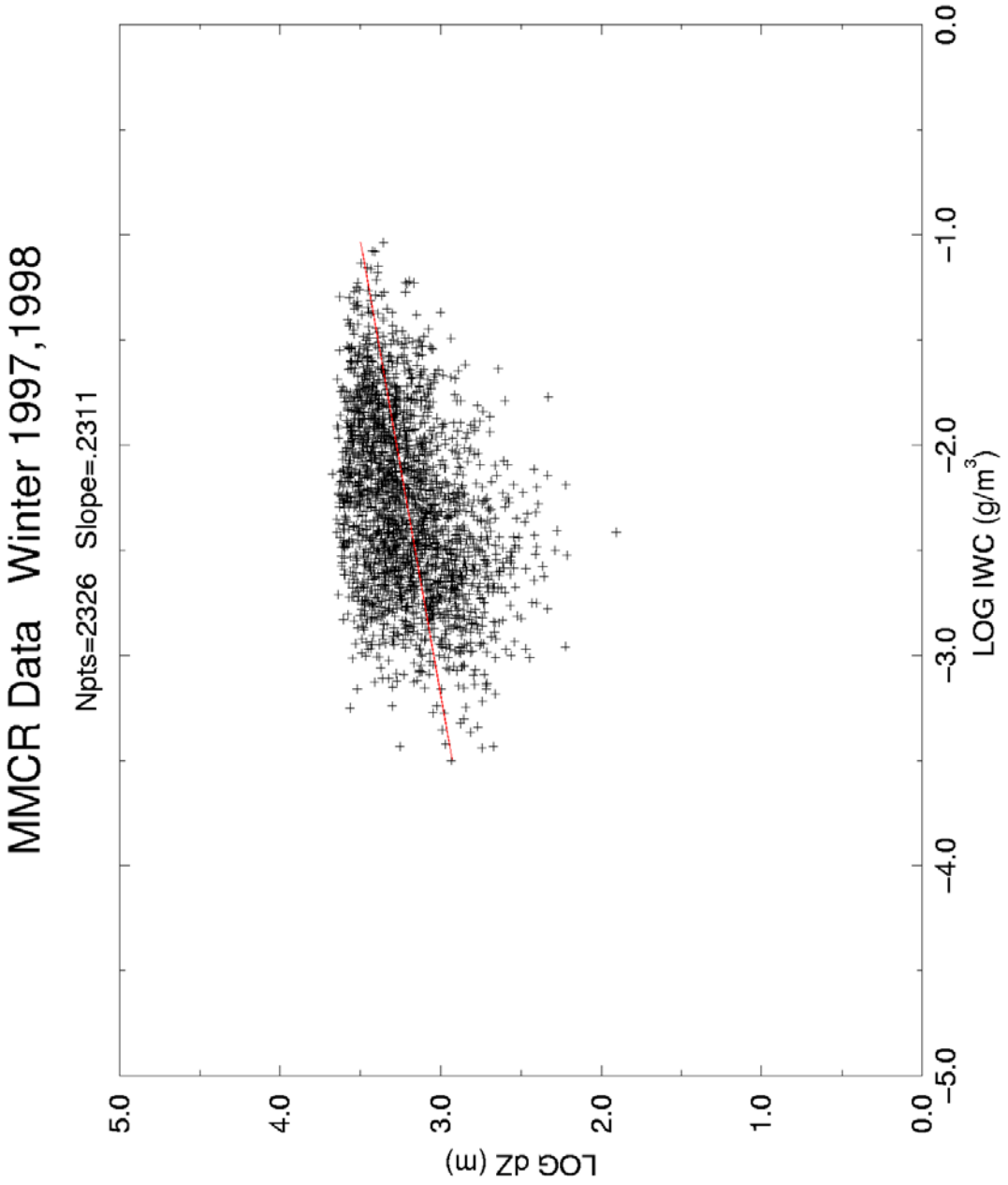

Figure 6(b). As in Figure 5b but for cirrus cloud physical thickness versus IWC.

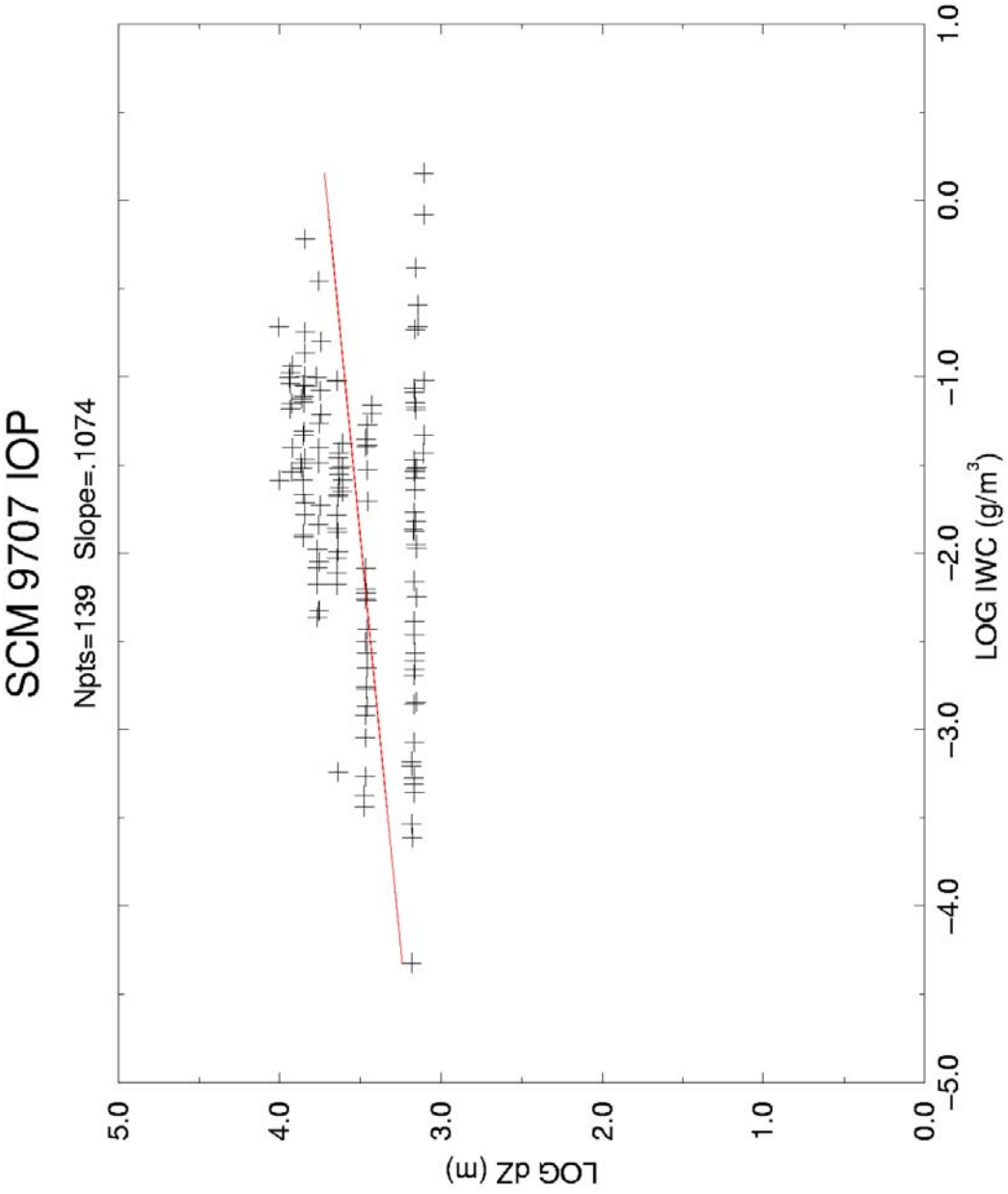

Figure 6(c). As in Figure 5c but for cirrus cloud physical thickness versus IWC.

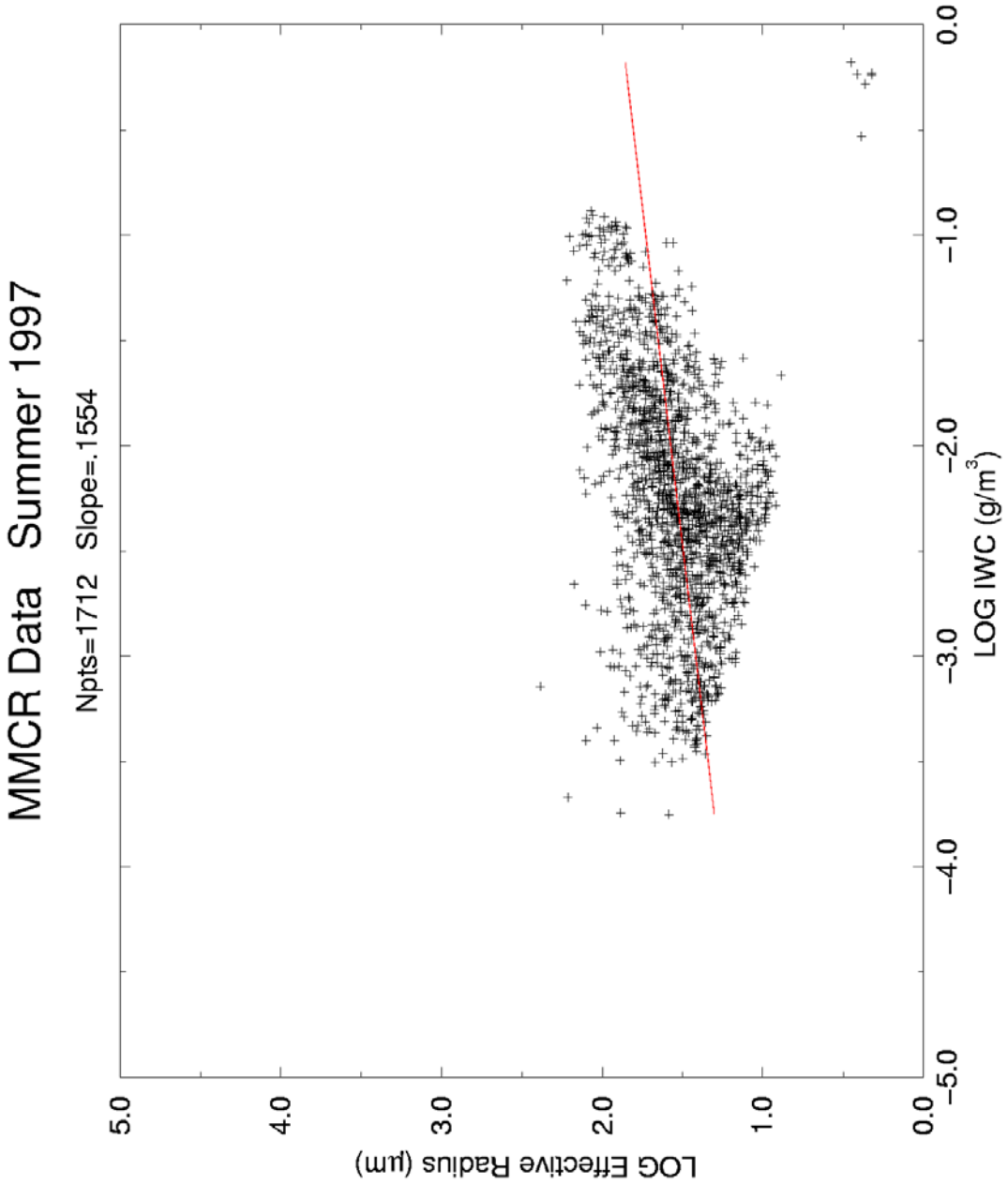

Figure 7(a). As in Figure 5a but for cirrus crystal effective radius versus IWC.

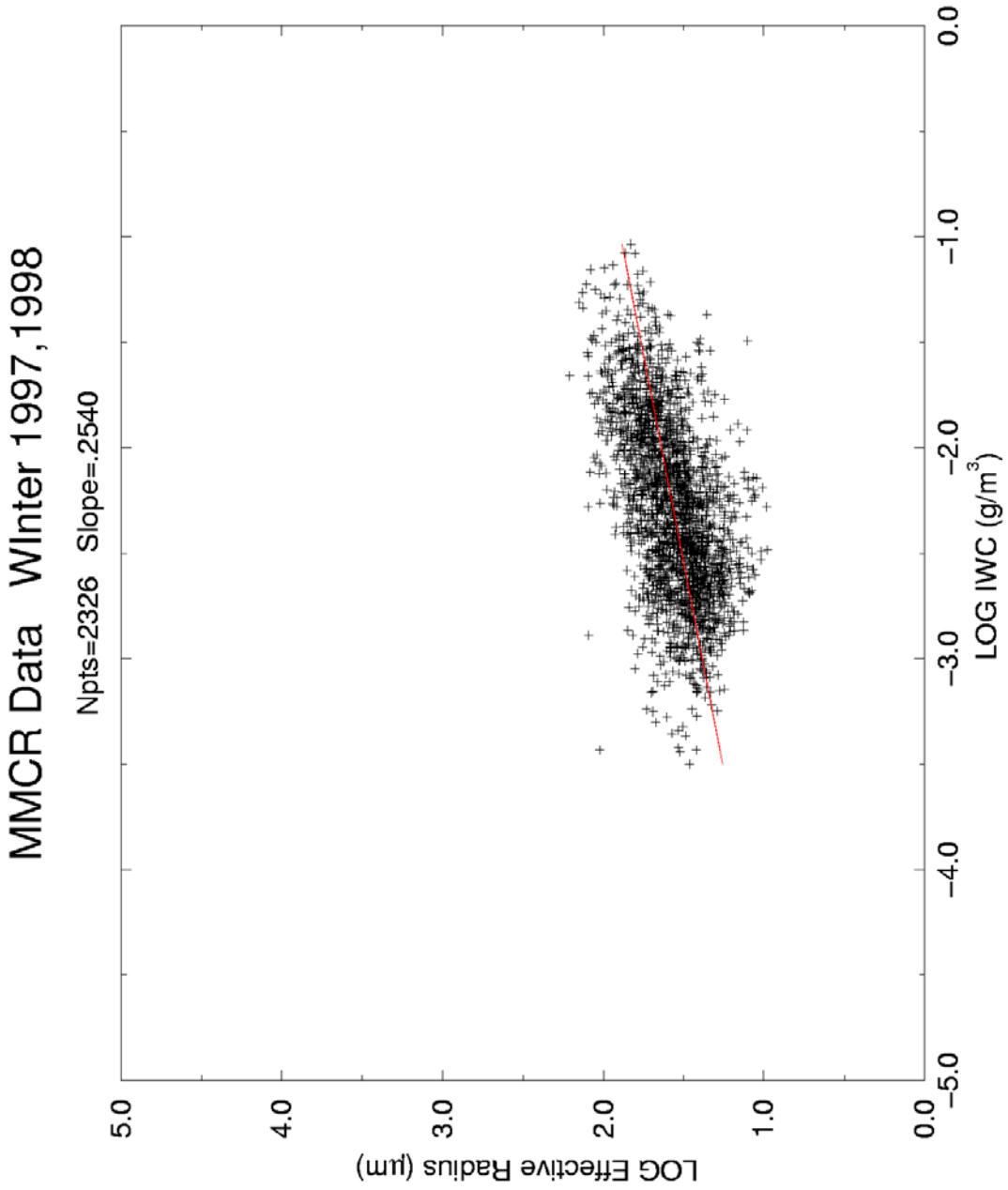

Figure 7(b). As in Figure 5b but for cirrus crystal effective radius versus IWC.

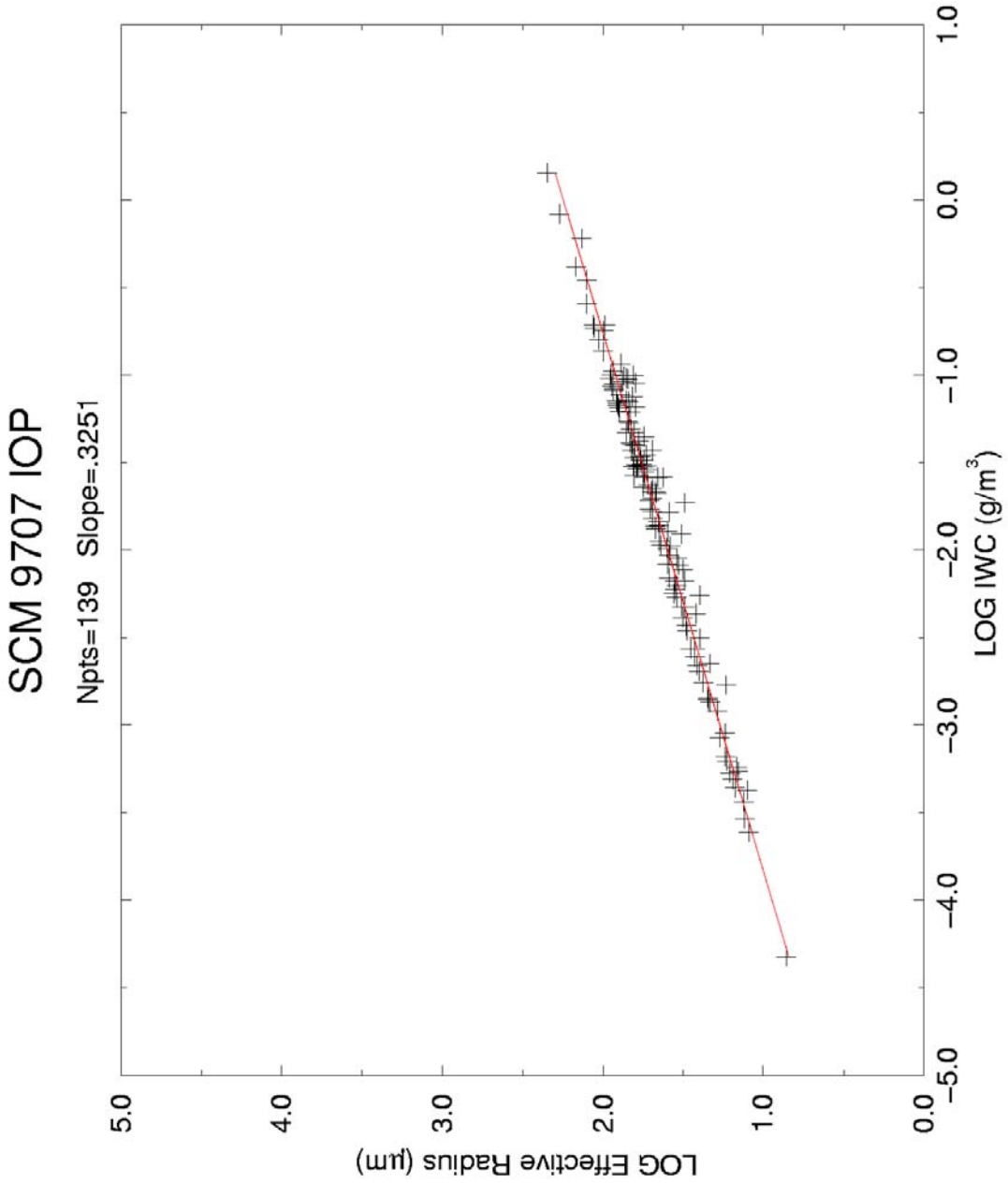

Figure 7(c). As in Figure 5c but for cirrus crystal effective radius versus IWC.